BIOCHEMISTRY
including biophysical chemistry & molecular biology
Article

Biochemistry **2010,** *49,* 10137–10145 10137
DOI: 10.1021/bi101700e

Mass Spectrometric Identification of Phosphorylation Sites in Guanylyl Cyclase A and B[†]

Andrea R. Yoder,[‡] Matthew D. Stone,[§] Timothy J. Griffin,[§] and Lincoln R. Potter*[,‡,§]

[‡]*Departments of Pharmacology and* [§]*Biochemistry, Molecular Biology, and Biophysics, University of Minnesota, Minneapolis, Minnesota 55455, United States*

Received July 2, 2010; Revised Manuscript Received October 26, 2010

ABSTRACT: Guanylyl cyclase A and B (GC-A and GC-B) are transmembrane guanylyl cyclase receptors that mediate the physiologic effects of natriuretic peptides. Some sites of phosphorylation are known for rat GC-A and GC-B, but no phosphorylation site information is available for the human homologues. Here, we used mass spectrometry to identify phosphorylation sites in GC-A and GC-B from both species. Tryptic digests of receptors purified from HEK293 cells were separated and analyzed by nLC-MS-MS. Seven sites of phosphorylation were identified in rat GC-A (S497, T500, S502, S506, S510, T513, and S487), and all of these sites except S510 and T513 were observed in human GC-A. Six phosphorylation sites were identified in rat GC-B (S513, T516, S518, S523, S526, and T529), and all six sites were also identified in human GC-B. Five sites are identical between GC-A and GC-B. S487 in GC-A and T529 in GC-B are novel, uncharacterized sites. Substitution of alanine for S487 did not affect initial ligand-dependent GC-A activity, but a glutamate substitution reduced activity 20%. Similar levels of ANP-dependent desensitization were observed for the wild-type, S487A, and S487E forms of GC-A. Substitution of glutamate or alanine for T529 increased or decreased ligand-dependent cyclase activity of GC-B, respectively, and T529E increased cyclase activity in a GC-B mutant containing glutamates for all five previously identified sites as well. In conclusion, we identified and characterized new phosphorylation sites in GC-A and GC-B and provide the first evidence of phosphorylation sites within human guanylyl cyclases.

Natriuretic peptides are pleiotropic factors that regulate blood pressure, cardiac hypertrophy, long bone growth, and other functions (*1*). Atrial natriuretic peptide (ANP)[1] and B-type natriuretic peptide (BNP) are released from the heart in response to cardiac chamber stretch. Both peptides reduce cardiac stress by decreasing blood pressure and cardiac hypertrophy. C-type natriuretic peptide (CNP) is found in bone, endothelium, and neuronal tissues. It stimulates long bone growth, axonal path-finding, and vasorelaxation. The signaling receptor for ANP and BNP is guanylyl cyclase A (GC-A), also known as natriuretic peptide receptor A, and the signaling receptor for CNP is guanylyl cyclase B (GC-B), also known as natriuretic peptide receptor B. Both GC-A and GC-B are transmembrane guanylyl cyclases that catalyze the synthesis of cGMP upon ligand binding (*2*).

In contrast to most cell surface receptors, GC-A and GC-B are basally phosphorylated and are desensitized by dephosphorylation (*3*−*7*). Upon exposure to ligand, the receptors are initially activated, but prolonged ligand exposure causes concomitant dephosphorylation and desensitization (*6*). Initial metabolically labeling studies identified six phosphorylation sites in rat GC-A (S497, T500, S502, S506, S510, and T513) and five phosphorylation sites in rat GC-B (S513, T516, S518, S523, and S526) (*8*, *9*). Importantly, all of these phosphorylation sites were shown to regulate enzymatic activity because the mutation of any single residue to alanine reduced receptor phosphate content and natriuretic-dependent guanylyl cyclase activity without affecting protein levels or detergent-dependent guanylyl cyclase activity (*7*). Furthermore, mutation of multiple residues to alanine resulted in receptors that bound hormone but could not be activated (*7*, *8*). In contrast, conversion of the same residues to glutamate in GC-A yielded a hormonally responsive receptor that was resistant to short-term desensitization (*10*).

Although the initial tryptic phosphopeptide mapping experiments identified several phosphorylation sites, we believe that additional sites remain to be discovered because highly homologous sea urchin guanylyl cyclases contain 15−17 mol of phosphate/receptor (*11*) whereas only five or six sites have been previously identified in GC-B and GC-A, respectively. Mass spectrometry provides direct chemical evidence of phosphorylation sites, which has never been demonstrated for GC-A or GC-B. Here, we used mass spectrometry to identify and characterize two new phosphorylation sites, chemically confirm previous identified sites, and identify phosphorylated residues in human natriuretic peptide receptors for the first time.

EXPERIMENTAL PROCEDURES

Reagents. PhosSelect affinity gel for immobilized metal affinity chromatography (IMAC), trypsin, and rat ANP were purchased from Sigma-Aldrich (St. Louis, MO); Empore SDB-XC disks were from 3M Corp. (St. Paul, MN).

Cell Lines. Human embryonic kidney 293 cells stably over-expressing rat or human GC-A or GC-B were maintained as previously described (*12*, *13*). Transient transfections were performed in cells that lack endogenous expression of any natriuretic peptide receptors (293neo cells) as previously described (*12*, *13*).

[†]This work was supported by NIH Grant R21HL0934402 to L.R.P.

*To whom correspondence should be addressed. Tel: 612-624-7251. Fax: 612-624-7282. E-mail: potter@umn.edu.

[1]Abbreviations: ANP, atrial natriuretic peptide; BNP, B-type natriuretic peptide; CNP, C-type natriuretic peptide; GC-A, guanylyl cyclase A; GC-B, guanylyl cyclase B; IMAC, immobilized metal affinity chromatography.

Published on Web 10/26/2010

Immunoprecipitation. Natriuretic peptide receptors were immunoprecipitated from cells stably overexpressing the desired receptor with antibodies that recognize the carboxyl terminal of GC-A or GC-B as previously described (*14*, *15*). Proteins were separated on Criterion gels by SDS−PAGE and visualized by Coomassie staining.

In-Gel Digestion. Protein bands of interest were excised from gels and digested with trypsin as described (*16*). Briefly, the excised band was cut into small pieces, dehydrated with acetonitrile (ACN), and treated with 1 mM DTT at 56 °C for 20 min to ensure reduction of cysteine residues. After another round of dehydration, samples were treated with 55 mM iodoacetamide in 100 mM NH_4HCO_3 to alkylate cysteine residues. The gel slices were again dehydrated with ACN and then rehydrated in a solution containing 12.5 ng/μL sequence-grade trypsin in 10 mM NH_4HCO_3 on ice for 2 h before incubation at 37 °C overnight. The tryptic peptides were then extracted from the gel with 1:2 solution of 5% formic acid:ACN in a 2-fold excess to the trypsin solution already present. After incubation at 37 °C for 30 min with shaking, the supernatant was then removed and dried by vacuum centrifugation.

Peptide Methylation. Methylation of free carboxyl groups was accomplished as follows (*17*). Forty microliters of acetyl chloride was added dropwise to 1 mL of anhydrous methanol and then used to resuspend the dried tryptic peptide sample. The mixture was then sonicated for 1 h at room temperature and allowed to further react for 30 min at room temperature before drying by vacuum centrifugation.

Phosphopeptide Enrichment and Sample Desalting. Immobilized metal affinity chromatography (IMAC) was used for phosphopeptide enrichment as described (*18*). Briefly, tryptic peptide samples were dissolved in 100 μL of IMAC binding buffer (40% ACN in 25 mM formic acid) and added to 10 μL of IMAC resin. The sample was incubated at room temperature with vigorous shaking for 1 h. The beads were then added to an equilibrated StageTip column (*19*) containing two 16-gauge needle punches of Empore SDB-XC disks. The IMAC resin was then washed with binding buffer to remove any nonspecifically bound peptides. Peptides specifically bound to the IMAC resin were eluted onto the Empore disks with excess K_2HPO_3, pH 7. Samples were then desalted, and the desired peptide fraction was eluted with 95% ACN in 0.1% trifluoacetic acid (TFA). Samples not enriched by IMAC were similarly desalted with StageTips. Sample eluates were dried by vacuum centrifugation.

Liquid Chromatography and Nanospray Mass Spectrometry. Liquid chromatography and mass spectrometry were performed essentially as described by Bandhakavi et al. (*20*) using an Eksigent 1DLC nanoHPLC in-line with an LTQ-Orbitrap XL (ThermoScientific) with a few exceptions. The gradient was 2−40% ACN in 0.1% formic acid over 60 min with a constant flow of 250 nL/min. Spray voltage was set to 1.95 kV, the heated capillary was set at 160 °C, and the tube lens voltage was set to either 145 or 65 V (the lower value was used to limit any potential phosphate loss). Full scans were performed in the orbital trap over a range of m/z 360−1800. Tandem mass spectra were scanned from the linear ion trap using collision-induced dissociation with a normalized collision energy of 35%, an isolation width of m/z 2.0, and target values of 10000 ions or 100 ms. A parent mass list was incorporated containing m/z values of candidate phosphopeptides with +2, +3, and +4 ionization states. The five most intense ions were selected for fragmentation. If a specific parent was not detected, the most intense ions not on the parent mass list were selected as a default. Dynamic exclusion was set for 20 s using the maximum of 500 entries and a mass window of −0.6 to 1.2 amu.

Mutagenesis. Site-directed mutagenesis of rat GC-A and GC-B was accomplished using the QuickChange II system (Stratagene, Cedar Creek, TX) as previously described (*7*). All mutations were confirmed by DNA sequencing.

Guanylyl Cyclase Assays. Crude membranes were prepared as described (*21*). Guanylyl cyclase assays were performed at 37 °C for 5 min in a buffer containing 25 mM Hepes, pH 7.4, 50 mM NaCl, 0.1% BSA, 0.5 mM 1-methyl-3-isobutylxanthine, 1 mM GTP, 0.5 μM microcystin, 1 mM EDTA, and 1−2 μCi of [α-^{32}P]GTP, with either 5 mM $MgCl_2$, 1 mM ATP, and 10 nM or 1 μM natriuretic peptide or 1% Triton X-100 with 5 mM $MnCl_2$ being substituted for the $MgCl_2$. Reactions were started by the addition of 80 μL of the above reagents to 50−200 μg of crude membrane protein suspended in 20 μL of phosphatase inhibitor buffer. Reactions were stopped by the addition of 0.5 mL of 110 mM ZnOAc and 0.5 mL of 110 mM $NaCO_3$ on ice. ^{32}P-cGMP was purified and detected as described previously (*22*).

Homologous Desensitization Assay. Cells expressing the desired receptor were incubated at 37 °C for 1 h in the presence or absence of either 100 nM or 1 μM ANP in DMEM. Cells were then washed twice with ice-cold PBS, and then membranes were prepared and assayed for guanylyl cyclase activity as described above.

Data Analysis. MS data were searched using the Proteome Discoverer 1.0 software pipeline using SEQUEST (ThermoScienific). Monoisotopic precursor and fragment ion tolerances were set to 10 ppm and 0.8 amu, respectively. Dynamic modifications of oxidation of Met and phosphorylation of Ser and Thr and the static modification of carbamidomethylation of Cys were selected. The databases used for searching were the rat international protein index (IPI) 20081024 v3.50 (40359 entries) or NCBI human v200806 (38126 entries). The SEQUEST discrimanant score (XCorr) and precursor mass error (ΔM) values reported here were determined by the software package. Numbering of sites of phosphorylation in human receptors is based on numbering of previously identified sites in the rat homologues.

Statistical Analysis. Statistical analysis of the guanylyl cyclase data was performed with GraphPad Prism software. All p-values were obtained using an unpaired t test where ≤ 0.05 was considered significant.

RESULTS

Identification of Known Phosphorylation Sites in Rat and Human GC-A and GC-B. Rat and human forms of GC-A and GC-B were purified from HEK 293 cells by sequential immunoprecipitation−SDS−PAGE fractionation (Supporting Information Figure S1). Gel slices containing the receptor of interest were then subjected to in-gel tryptic digestion, and resulting peptides were extracted. In some experiments, free carboxylic acid groups in the peptides were methylated, and/or the phosphopeptides were enriched by immobilized metal affinity chromatography (IMAC). The peptide mixtures were then submitted to nLC-MS-MS, and the resulting mass/charge data were searched against the appropriate IPI rat or NCBI human database. In the database analysis of GC-A and GC-B phosphopeptides, the peptide species noted at the top of the spectra indicate the best possible match from all possible theoretical

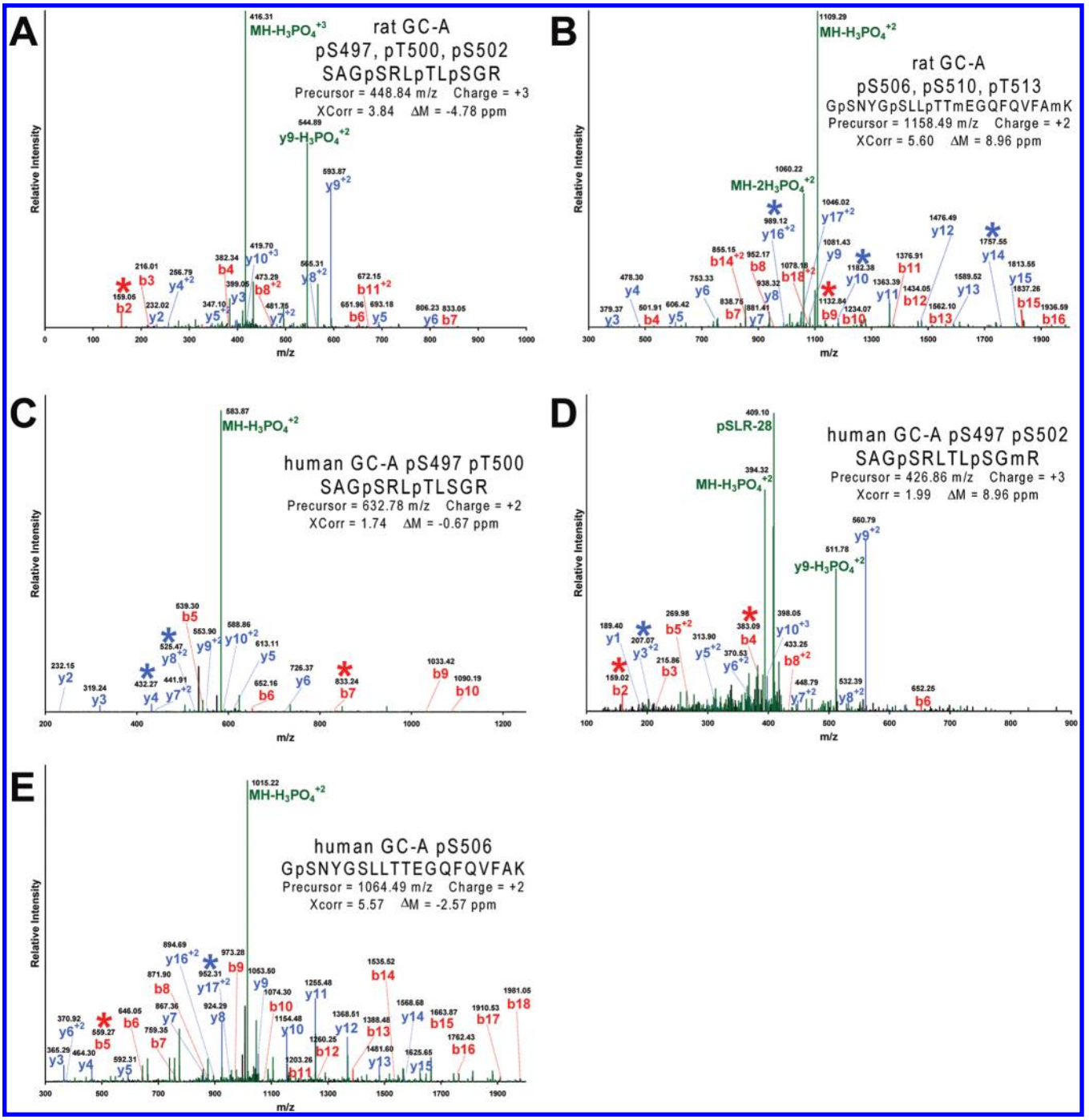

FIGURE 1: Tandem mass spectrometric spectra depicting phosphorylated residues in rat GC-A and human GC-A. Receptors were purified and digested with trypsin prior to analysis by tandem mass spectrometry. Spectra for each phosphopeptide are color coded for matched b- and y-ions in red and blue, respectively. Other matches to the theoretical fragmentation are shown in green. For clarity, only selected species are labeled within the spectra. The primary amino acid sequence for each phosphorylated peptide is denoted on each spectrum and all b- and y-ions matched from the spectrum are marked. Lowercase letters directly preceding amino acids indicate modifications (p = phosphorylated; m = methylated; o = oxidized). Precursor ion m/z value and charge state are listed for the spectrum. SEQUEST discriminant score (XCorr) and mass error (ΔM) values reported for the spectrum were determined by the Proteome Discoverer software. Asterisks indicate ions that support the phosphorylation of specific serines or threonines. (A) Tandem mass spectrum identifying pS497, pT500, and pS502 within rat GC-A. (B) Tandem mass spectrum identifying pS506, pS510, and pT513 within rat GC-A. (C) Tandem mass spectrum identifying pS497 and pT500 within human GC-A. (D) Tandem mass spectrum identifying pS497 and pS502 within human GC-A. (E) Tandem mass spectrum identifying pS506 within human GC-A.

tryptic peptides in the entire rat or human protein database of 40359 or 38126 proteins, respectively. In other words, when no constraints were set upon the system, the search algorithms determined that the best match for the spectrum was a specific phosphorylated peptide from GC-A or GC-B. In addition, all sites of modification were confirmed by manual inspection of MS/MS spectra.

All six previously identified phosphorylation sites in rat GC-A (*9*) were identified by mass spectrometry. Due to the fact that GC-A contains 6 known sites within a 17 amino acid span, peptides containing multiple phosphorylated residues were observed. Panels A and B of Figure 1 illustrate MS/MS spectra consistent with the triply phosphorylated peptides SAGpSRLpTLpSGR and GpSNYGpSLLpTTmEGQFQVFAmK, respectively, where

lowercase letters indicate a modification to the amino acid which they precede (p = phosphorylation; m = methylation; o = oxidation). Please note that b-series ions and y-series ions from the MS/MS analysis are depicted as red or blue peaks, respectively, and that larger, more detailed, spectra are shown in Supporting Information Figures S2−S16. The first peptide contains a missed trypsin cleavage site, which often results when a phosphothreonine or phosphoserine is two residues C-terminal to an arginine or lysine (*7*). Green peaks indicate additional matches to the theoretical fragmentation pattern. XCorr and ΔM values, as determined by the Proteome Discoverer software, are listed on each spectrum. Xcorr is the score for the match with higher values indicating a greater likelihood that the peak is the predicted peptide. ΔM reflects the accuracy of the peptide mass measurement with lower values indicating a more precise measurement. Asterisks indicate key ions that determine which residues in the phosphopeptides are actually phosphorylated. For instance in Figure 1A, the presence of the b2 and y9 ions indicates a triply phosphorylated peptide containing phosphates likely on S497, T500, and S502. Likewise, in Figure 1B the concurrent presence of the y10, y16, b9, and y14 ions indicates phosphorylation occurs at S506, S510, and T513. Together, these two phosphopeptides contain all six known rat GC-A phosphorylation sites (S497, T500, S502, S506, S510, and T513). Spectra describing mono- and diphosphorylated versions of these peptides were observed as well but are not presented due to space limitations.

MS/MS analysis of tryptic digestions of human GC-A revealed mass/charge species corresponding to the diphosphorylated peptides SAGpSRLpTLSGR (Figure 1C) and SAGpSRLTLpSGmR (Figure 1D). The presence of the y4 and y8 ions in Figure 1C in conjunction with the presence of b7 indicates phosphorylation at S497 and T500 in this peptide. In Figure 1D, the presence of the b2, b4, and y3 ions suggests phosphorylation at S497 and S502. The monophosphorylated peptide GpSNYGSLLTTEGQFQVFAK was also identified (Figure 1E), where the presence of the b5 ion in conjunction with the y17 ion indicates phosphorylation at S506. We did not observe peptides containing phosphorylated versions of S510 or T513 in human GC-A. However, the corresponding nonphosphorylated versions of these peptides also were not found when omitting the phosphopeptide enrichment step, suggesting that lack of identification may result from inability to detect the relevant peptides by mass spectrometry. Thus, for the first time, we determined that human GC-A is phosphorylated on residues corresponding to S497, T500, S502, and S506 in rat GC-A.

MS/MS analysis of proteolytic samples of rat GC-B identified all five previously known phosphorylation sites. Figure 2A illustrates a spectrum depicting the phosphopeptide GAGpSRLpTLSLR. The presence of both the y3 and b7 ions confirms phosphorylation at S513 and T516. The singly phosphorylated peptide LTLpSLR (Figure 2C) was phosphorylated on S518 as indicated by the presence of the y4 ion. Figure 2E depicts the spectrum of GSpSYGpSLoMTAHGK, which is phosphorylated at both S523 and S526, as indicated by the presence of the y11, y10, and y7 ions. These three phosphopeptides account for all previously known rat GC-B phosphorylation sites (S513, T516, S518, S523, and S526).

MS/MS analysis of tryptic digests of human GC-B revealed the phosphopeptides GAGpSRLpTLSLR (Figure 2B), LTLpSLR (Figure 2D), and GSpSYGpSLoMTAHGK (Figure 2E). In Figure 2B, the presence of the y4 and b7 ions indicates phosphorylation at S513 and T516. The presence of the y4 ion in Figure 2D suggests phosphorylation at S518. As can be seen in Figure 2F, the presence of the y11, y10, y7, b5, and y8 ions are consistent with phosphorylation at S523 and S526. Thus, for the first time, we have shown that human GC-B is phosphorylated on sites corresponding to S513, T516, S518, S523, and S526 in rat GC-B.

Identification of Novel Phosphorylation Sites in Rat and Human GC-A. A novel phosphorylation site at S487 was also identified in GC-A. MS/MS spectra containing peaks corresponding to the mass/charge ratio of the peptides WEDLQPSpSLER and WEDVEPSpSLER were identified in the proteolytic digest of rat and human GC-A, respectively (Figure 3A,B). In both spectra, the presence of the b7 and y4 ions indicates phosphorylation at S487. To investigate the function of this phosphorylation site, we created mutants expressing an alanine or glutamate at position 487 in rat GC-A. One micromolar ANP stimulated the guanylyl cyclase activity of GC-A to 76%, 67%, and 61% of the activity measured in the presence of 1% Triton X-100 and Mn^{2+}GTP in membranes from cells transfected with wild-type, S487A, and S487E GC-A constructs, respectively (Figure 3C). The 20% reduction in the S487E compared to wild-type GC-A was statistically significant.

The effect of S487 phosphorylation on ANP-dependent desensitization of GC-A was investigated by incubating 293 cells expressing wild type or S487 mutants with ANP for 1 h at 37 °C prior to membrane preparation. ANP-dependent and detergent-dependent guanylyl activities in the resulting membranes were then determined and expressed as ratios of ANP-dependent activity/detergent-dependent activity to control for transfection efficiencies and expression levels. Relative desensitization was determined by expressing cyclase activities measured in membranes from ANP-exposed cells as a percentage of activities measured in membranes from cells not exposed to ANP. Prior exposure to 1 μM ANP reduced hormone-dependent cyclase activity by 52%, 48%, and 62% in membranes from cells expressing wild-type, S487A, and S487E versions of GC-A (Figure 3D). The reductions in activity were not significantly different from one another at $p < 0.05$.

Whole cell desensitization with 10-fold less ANP (100 nM) yielded similar results. Cyclase activities measured in the presence of 1 μM ANP were reduced by 50%, 51%, and 27% in membranes from cells expressing wild-type, S487A, and S487E versions of GC-A (Figure 3E). The amount of desensitization seen in GC-A S487E was statistically less than that of wild-type GC-A or GC-A S487A ($p = 0.008$ and $p = 0.016$, respectively). Reductions in hormone-dependent cyclase activity determined in the presence of 10 nM ANP were 48%, 45%, and 23% in membranes from cells expressing wild-type, S487A, and S487E versions of GC-A, respectively, and were not significantly different from one another.

Identification of a Novel Phosphorylation Site in Rat and Human GC-B. In addition to the five previously identified phosphorylation sites of GC-B, our mass spectrometric analysis indicated that GC-B was also phosphorylated at T529. Peaks representing the singly and doubly phosphopeptides GSSYGSLoMpTAHGK and GSpSYGSLoMpTAHGK were observed in spectra from tryptic digests of rat and human GC-B, respectively (Figure 4A,B). In Figure 4A, the presence of the b7 and y6 ions indicates phosphorylation of the T529 residue. In Figure 4B, the presence of the y11 and y10 ions in conjunction with the b3 and y5 ions is consistent with phosphorylation at S523 and T529.

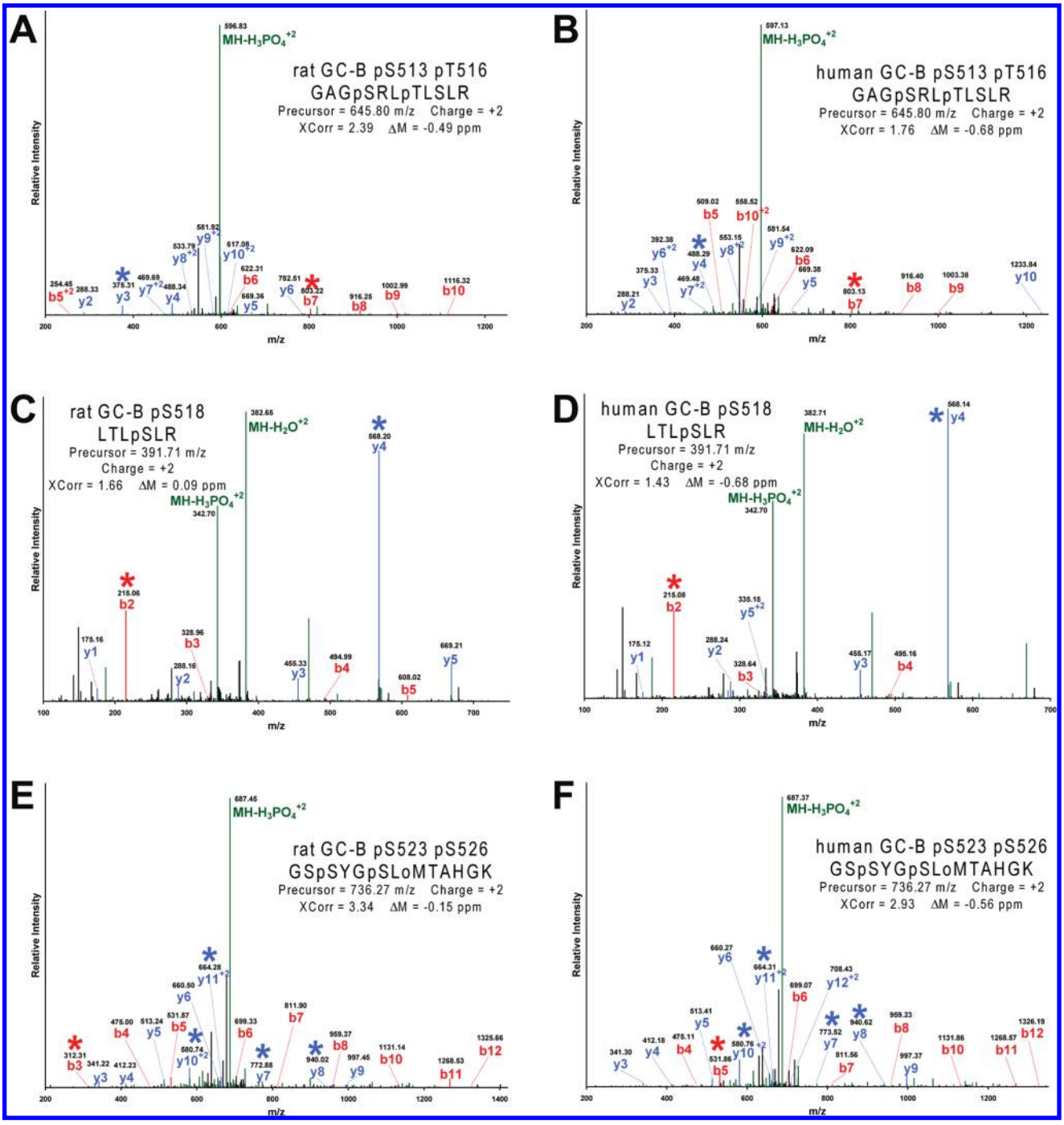

FIGURE 2: Tandem mass spectrometric spectra depicting phosphorylated residues in rat and human GC-B. Spectra were generated and are labeled as described in Figure 1. (A) Tandem mass spectrum identifying pS513 and pT516 within rat GC-B. (B) Tandem mass spectrum identifying pS513 and pT516 within human GC-B. (C) Tandem mass spectrum identifying pS518 within rat GC-B. (D) Tandem mass spectrum identifying pS518 within human GC-B. (E) Tandem mass spectrum identifying pS523 and pT526 within rat GC-B. (F) Tandem mass spectrum identifying pS523 and pT526 within human GC-B.

T529 in GC-B is homologous to T513 in GC-A, which is a known phosphorylation site (Figure 5B). To investigate the functional consequence of phosphorylation at T529, we mutated T529 in wild-type rat GC-B to alanine or glutamate and measured CNP-dependent guanylyl cyclase activity in membranes from cells transiently expressing each receptor. The alanine, but not the glutamate, mutation decreased hormone-dependent cyclase activity (Figure 4C). In addition, the T529E mutation was introduced into a receptor containing glutamate substitutions at all five previously identified phosphorylation sites (GC-B-5E) (*23*, *24*) to generate a receptor containing six glutamates (GC-B-6E). CNP-dependent guanylyl cyclase activity was significantly higher in membranes from cells expressing GC-B-6E compared to cells expressing GC-B-5E (Figure 4D). Together, these data indicate that phosphorylation of threonine 529 is required for maximum CNP-dependent guanylyl cyclase activity of GC-B.

DISCUSSION

The veracity of these phosphopeptide identifications is supported in two ways. First, the MS/MS spectra matched to phosphopeptides from GC-A or GC-B that were obtained by

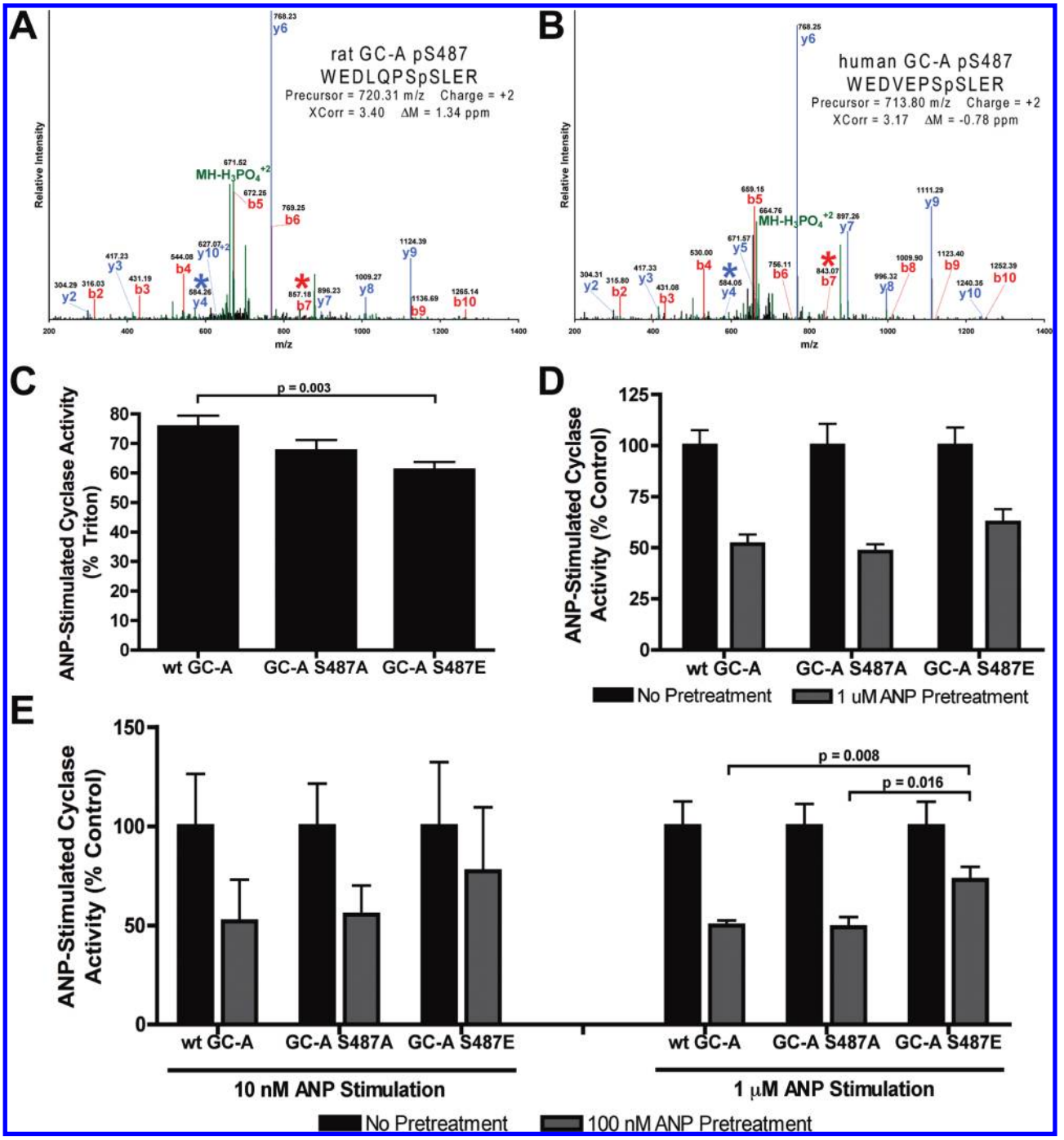

FIGURE 3: Mass spectroscopic identification of phosphorylated Ser-487 in rat and human GC-A and functional characterization of Ser-487 in rat GC-A. Spectra were generated and are labeled as described in Figure 1. (A) Tandem mass spectrum identifying pS487 in rat GC-A. (B) Tandem mass spectrum identifying pS487 in human GC-A. (C) Guanylyl cyclase activities in membranes of 293 cells expressing wild-type or mutant forms of rat GC-A where $n = 25$. Assays were conducted in the presence of either 1 μM ANP or 1% Triton X-100. Results are normalized to the maximum cGMP concentrations obtained in the presence of Triton X-100. (D) Homologous desensitization assessed by guanylyl cyclase activities in 293 cells expressing wild-type or mutant forms of rat GC-A preincubated with 1 μM ANP for 1 h. Assays were conducted in the presence of either 1 μM ANP or 1% Triton X-100. Results are expressed as the activation ratio of ligand-stimulated activity divided by activity determined in the presence of 1% Triton-X 100 and Mn^{2+} GTP, which were then normalized to the nonpretreated control for each receptor where $n = 8$. (E) Homologous desensitization assessed by guanylyl cyclase activities in 293 cells expressing wild-type or mutant forms of rat GC-A preincubated with 100 nM ANP for 1 h. Assays were conducted in the presence of either 10 nM ANP, 1 μM ANP, or 1% Triton X-100. Results are expressed as the activation ratio of ligand-stimulated activity divided by activity determined in the presence of 1% Triton-X 100 and Mn^{2+} GTP, which were then normalized to the nonpretreated control for each receptor where $n = 6$.

searching against databases containing approximately 40000 protein sequences, so the probability of these MS/MS peaks randomly matching the expected proteins is absurdly low. Second, regarding the issue of determining the exact site or sites of modification, we manually evaluated the MS/MS spectra from each phosphopeptide, and in all cases, we confirmed that the sites of phosphorylation determined by sequence database searching were supported by the peptide fragmentation pattern. Thus, the modification sites presented are well supported by the mass spectrometry data.

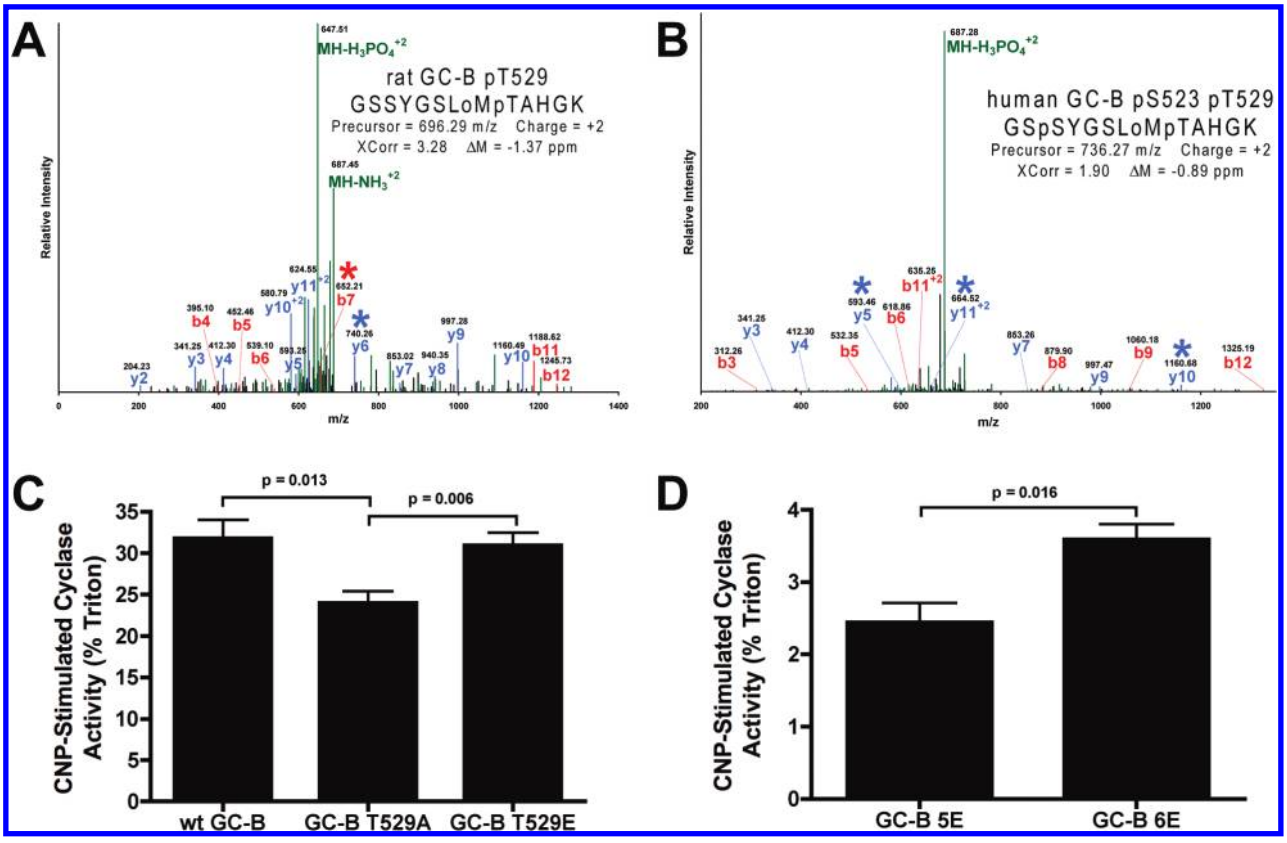

FIGURE 4: Mass spectroscopic identification of phosphorylated Thr-529 in rat and human GC-B. Spectra were generated and are labeled as described in Figure 1. (A) Tandem mass spectrum identifying pT529 in rat GC-B generated from a tryptic digest of rat GC-B. (B) Tandem mass spectrum identifying pS523 and pT529 in human GC-B. (C) Guanylyl cyclase activities from membranes obtained from 293 cells expressing rat wild-type GC-B with T529 mutated to either alanine or glutamic acid where $n = 8$. (D) Guanylyl cyclase activities from membranes obtained from 293 cells expressing either rat GC-B containing glutamic acid substitutions at all five previously known phosphorylated residues (GC-B-5E) or rat GC-B with a glutamic acid residue substitution at T529 in addition to previously known sites (GC-B-6E) where $n = 4$. Cyclase activities were determined in the presence of 1 μM CNP or 1% Triton X-100. Results are normalized to the maximum cGMP concentrations obtained in the presence of Triton X-100.

As a result of these methods, a total of seven phosphorylation sites within rat GC-A and six phosphorylation sites in rat GC-B were identified. A summary of known GC-A and GC-B phosphorylation sites and how they were detected is shown in Figure 5A. Of the GC-A sites, five were found in both the rat and human forms. Of the GC-B sites, all six were found in both rat and human forms. Five of the GC-B phosphorylation sites are conserved in GC-A. Mass spectrometric evidence was obtained for all sites that were originally identified by tryptic phosphopeptide mapping of ^{32}P-labeled receptors (*7*, *8*). In addition, evidence for one new site in GC-A (S487) and one new site in GC-B (T529) was obtained. The amino acid corresponding to S487 in GC-A is an asparagine in GC-B; thus phosphorylation of S487 is unique to GC-A.

During the course of our studies, Schroter and colleagues published a report documenting phosphorylation sites in FLAG-tagged rat GC-A using mass spectroscopy techniques (*25*). In agreement with the information presented here, they detected phosphorylation at S487, S497, T500, S502, S506, S510, and T513 of rat GC-A overexpressed in 293 cells. They also detected phosphorylation of S487, S497, and T500 in primary endothelial cells, which is impressive given the low levels of GC-A expression in these cells. They did not analyze sites in human GC-A or any form of GC-B. Consistent with our data, they observed less ANP-dependent cyclase activity in membranes from cells expressing GC-A-S487E compared to the wild-type receptor. However, they observed a 35% decrease in activity whereas we saw a 20% decrease. Schroter and colleagues did not measure desensitization of the S487A receptor. We do not know the reason for the difference in scale of the decrease observed by the two groups, but we note that ANP was present at 10-fold higher concentration in our guanylyl cyclase assay.

One major assertion of Schroter and co-workers was that phosphorylation of S487 is necessary for the homologous desensitization of rat GC-A. In fact, it was suggested to directly cause the decrease in activity seen in response to pretreatment with ligand. This conclusion was based on two major findings. First, they found that activity of the glutamate mutant was not blunted in response to 1 h pretreatment with 100 nM ANP. Second, they found that the relative ratio of tryptic phosphorylated to dephosphorylated peptides containing S487 increased approximately 9.5-fold upon ANP pretreatment as determined by semiquantitative mass spectrometry. However, the hypothesis that phosphorylation of S487 is required for homologous desensitization of GC-A is in direct conflict with our data demonstrating that S487A and S487E mutant receptors desensitize similarly to the wild-type receptor (Figure 3D).

One difference between our studies and those of Schroter and colleagues is the concentration of ligand used for homologous desensitization studies. In our protocol, cells are pretreated and assayed for guanylyl cyclase activity with a maximally stimulating concentration of ANP (1 μM). Schroter and co-workers pretreated cells with 100 nM ANP and assayed activities in the presence of 10 nM ANP, which can be problematic due to ANP

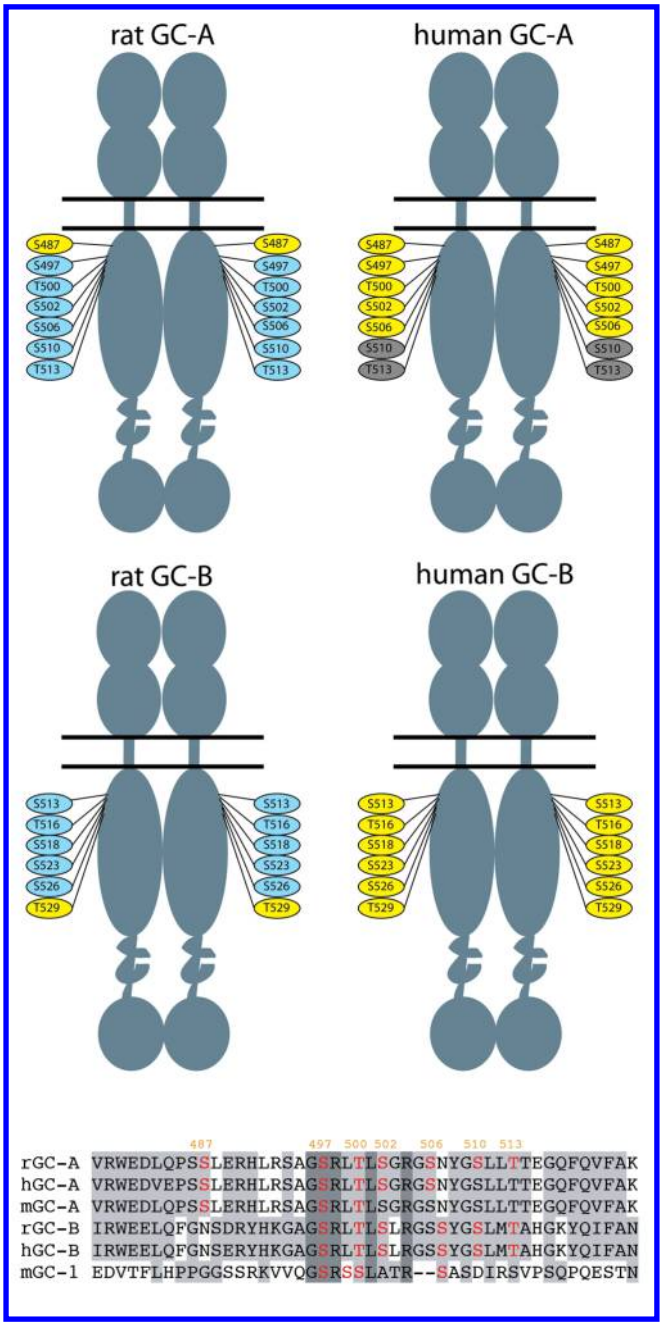

FIGURE 5: Identified phosphorylation sites in mammalian particulate guanylyl cyclases. (top and middle panels) Schematic of the rat and human membrane-bound natriuretic peptide receptors illustrating known phosphorylated residues. Phosphorylation sites are identified both by residue number and by identification procedure. Blue residues were identified both by ^{32}P-phosphopeptide mapping and by mass spectrometry. Yellow residues were identified by mass spectrometry only. Gray residues are predicted to be phosphorylated by sequence homology to known phosphorylated residues. (bottom panel) Sequence alignment of phosphorylated regions from mouse (m), rat (r), and human (h) homologues of GC-A, GC-B, and retinal guanylyl cyclase (GC-1). Positions where structurally similar residues are conserved in two or more proteins are shaded in light gray. Residues conserved in all proteins are shaded in dark gray. Red residues indicate identified phosphorylation sites. Numbers on the top line refer to rat GC-A sites. The alignment was performed with ClustalW.

carryover from whole cell exposure. To determine if the unique desensitization protocols explain the differing results, we investigated homologous desensitization using conditions described by Schroter et al. (Figure 3E). Reductions in ANP-dependent cyclase activities were observed with wild-type as well as S487A and S487E versions of GC-A when stimulated with 10 nM or 1 μM ANP. In all assays, S487E desensitized less than the wild-type or S487A receptor, and in studies involving pretreatment with 100 nM ANP and assaying with 1 μM ANP, these differences were significant. Regardless, we observed homologous desensitization of both the S487A and S487E GC-A using our original homologous desensitization protocol as well as the protocol described by Schroter et al., and therefore, conclude that phosphorylation of S487 is not required for homologous desensitization of GC-A.

It is clear that phosphorylation of S487 in GC-A does not have the same effect on cyclase activity as the previously identified sites. The small magnitude of the changes seen with these mutants decreases confidence that phosphorylation of S487 regulates GC-A guanylyl cyclase activity. Whether the *in vivo* regulatory effect of phosphorylation of S487 is to modulate cyclase activity or some other function is not known at the moment, but the marginal effect on cyclase activity is suggestive of other functions.

Recent studies by Bereta et al. have demonstrated phosphorylation at four serine residues within the kinase homology domain of guanylyl cyclase 1 (GC1) (also known as GC-E) from mouse retina using mass spectrometry (*26*). Interestingly, the four phosphorylation sites identified within the kinase homology domain of GC1 align with the highly phosphorylated region of the kinase homology domains of GC-A and GC-B. In fact, two of the GC1 phosphorylation sites (S530 and S533) align exactly with the phosphorylation sites in GC-A/B reported here (S497/513 and T500/516) (Figure 5B). However, unlike the phosphorylation sites in the same region of GC-A and GC-B, mutation of the phosphorylation sites in GC1 to either alanine or glutamic acid had no effect on guanylyl cyclase activity. Thus, other members of the guanylyl cyclase family have phosphorylation sites that do not greatly affect cyclase activity, which is similar to what we observed regarding S487 in GC-A.

Finally, it is unclear whether additional sites of phosphorylation remain to be determined in GC-A and GC-B. Although mass spectrometry is a very sensitive and accurate technique, if the phosphopeptides do not enter the instrument, they will not be identified. Previous studies with ^{32}P-labeled peptides indicated that most of the radioactivity (~90%) was lost in the preparation procedure (*9*). In the current study, we have no way of measuring phosphopeptide loss since the initial protein was not labeled. In addition, some peptides ionize poorly for unknown reasons, and therefore, will not be detected. Thus, we are confident in the positive identification of current sites but cannot exclude the possibility that additional phosphorylation sites remain to be determined.

In conclusion, we have identified seven phosphorylation sites (S487, S497, T500, S502, S506, S510, and T513) in rat GC-A and five phosphorylation sites (S487, S497, T500, S502, and S506) in human GC-A by mass spectrometry. Six identical phosphorylated residues (S513, T516, S518, S523, S526, and T529) were biochemically identified in rat and human GC-B. These studies lay the foundation for future analysis of phosphorylation-dependent regulation of rat and human guanylyl cyclase receptors.

ACKNOWLEDGMENT

We thank the Center for Mass Spectrometry and Proteomics facility at the University of Minnesota for instrumentation support and the Minnesota Supercomputing Institute for computational hardware and software support.

SUPPORTING INFORMATION AVAILABLE

One figure demonstrating the specificity of the antibodies used for immunoprecipitation (Figure S1) and larger, more detailed versions of all MS/MS spectra presented here (Figures S2−S16) with each spectrum accompanied by a detailed b- and y-ion fragmentation table highlighting matched fragments is included in the supporting information. This material is available free of charge via the Internet at http://pubs.acs.org.

REFERENCES

1. Potter, L. R., Yoder, A. R., Flora, D. R., Antos, L. K., and Dickey, D. M. (2009) Natriuretic peptides: their structures, receptors, physiologic functions and therapeutic applications. *Handb. Exp. Pharmacol.,* 341–366.
2. Potter, L. R. (2009) Guanylyl cyclases, in Handbook of Cell Signaling (Bradshaw, R. A., and Dennis, E. A., Eds.) Academic Press, Oxford.
3. Potter, L. R. (1998) Phosphorylation-dependent regulation of the guanylyl cyclase-linked natriuretic peptide receptor B: dephosphorylation is a mechanism of desensitization. *Biochemistry 37*, 2422–2429.
4. Joubert, S., Labrecque, J., and De Lean, A. (2001) Reduced activity of the NPR-A kinase triggers dephosphorylation and homologous desensitization of the receptor. *Biochemistry 40*, 11096–11105.
5. Koller, K. J., Lipari, M. T., and Goeddel, D. V. (1993) Proper glycosylation and phosphorylation of the type A natriuretic peptide receptor are required for hormone-stimulated guanylyl cyclase activity. *J. Biol. Chem. 268*, 5997–6003.
6. Potter, L. R., and Garbers, D. L. (1992) Dephosphorylation of the guanylyl cyclase-A receptor causes desensitization. *J. Biol. Chem. 267*, 14531–14534.
7. Potter, L. R., and Hunter, T. (1998) Phosphorylation of the kinase homology domain is essential for activation of the A-type natriuretic peptide receptor. *Mol. Cell. Biol. 18*, 2164–2172.
8. Potter, L. R., and Hunter, T. (1998) Identification and characterization of the major phosphorylation sites of the B-type natriuretic peptide receptor. *J. Biol. Chem. 273*, 15533–15539.
9. Potter, L. R., and Hunter, T. (1999) Identification and characterization of the phosphorylation sites of the guanylyl cyclase-linked natriuretic peptide receptors A and B. *Methods 19*, 506–520.
10. Potter, L. R., and Hunter, T. (1999) A constitutively "phosphorylated" guanylyl cyclase-linked atrial natriuretic peptide receptor mutant is resistant to desensitization. *Mol. Biol. Cell 10*, 1811–1820.
11. Ramarao, C. S., and Garbers, D. L. (1988) Purification and properties of the phosphorylated form of guanylate cyclase. *J. Biol. Chem. 263*, 1524–1529.
12. Dickey, D. M., Burnett, J. C., Jr., and Potter, L. R. (2008) Novel bifunctional natriuretic peptides as potential therapeutics. *J. Biol. Chem. 283*, 35003–35009.
13. Dickey, D. M., Yoder, A. R., and Potter, L. R. (2009) A familial mutation renders atrial natriuretic peptide resistant to proteolytic degradation. *J. Biol. Chem. 284*, 19196–19202.
14. Bryan, P. M., and Potter, L. R. (2002) The atrial natriuretic peptide receptor (NPR-A/GC-A) is dephosphorylated by distinct microcystin-sensitive and magnesium-dependent protein phosphatases. *J. Biol. Chem. 277*, 16041–16047.
15. Abbey, S. E., and Potter, L. R. (2002) Vasopressin-dependent inhibition of the C-type natriuretic peptide receptor, NPR-B/GC-B, requires elevated intracellular calcium concentrations. *J. Biol. Chem. 277*, 42423–42430.
16. Shevchenko, A., Tomas, H., Havlis, J., Olsen, J. V., and Mann, M. (2006) In-gel digestion for mass spectrometric characterization of proteins and proteomes. *Nat. Protoc. 1*, 2856–2860.
17. Ficarro, S. B., Salomon, A. R., Brill, L. M., Mason, D. E., Stettler-Gill, M., Brock, A., and Peters, E. C. (2005) Automated immobilized metal affinity chromatography/nano-liquid chromatography/electrospray ionization mass spectrometry platform for profiling protein phosphorylation sites. *Rapid Commun. Mass Spectrom. 19*, 57–71.
18. Villen, J., and Gygi, S. P. (2008) The SCX/IMAC enrichment approach for global phosphorylation analysis by mass spectrometry. *Nat. Protoc. 3*, 1630–1638.
19. Rappsilber, J., Mann, M., and Ishihama, Y. (2007) Protocol for micro-purification, enrichment, pre-fractionation and storage of peptides for proteomics using StageTips. *Nat. Protoc. 2*, 1896–1906.
20. Bandhakavi, S., Stone, M. D., Onsongo, G., Van Riper, S. K., and Griffin, T. J. (2009) A dynamic range compression and three-dimensional peptide fractionation analysis platform expands proteome coverage and the diagnostic potential of whole saliva. *J. Proteome Res. 8*, 5590–5600.
21. Antos, L. K., Abbey-Hosch, S. E., Flora, D. R., and Potter, L. R. (2005) ATP-independent activation of natriuretic peptide receptors. *J. Biol. Chem. 280*, 26928–26932.
22. Bryan, P. M., and Potter, L. R. (2002) The atrial natriuretic peptide receptor (NPR-A/GC-A) is dephosphorylated by distinct microcystin-sensitive and magnesium-dependent protein phosphatases. *J. Biol. Chem. 277*, 16041–16047.
23. Abbey-Hosch, S. E., Smirnov, D., and Potter, L. R. (2005) Differential regulation of NPR-B/GC-B by protein kinase C and calcium. *Biochem. Pharmacol. 70*, 686–694.
24. Potthast, R., Abbey-Hosch, S. E., Antos, L. K., Marchant, J. S., Kuhn, M., and Potter, L. R. (2004) Calcium-dependent dephosphorylation mediates the hyperosmotic and lysophosphatidic acid-dependent inhibition of natriuretic peptide receptor-B/guanylyl cyclase-B. *J. Biol. Chem. 279*, 48513–48519.
25. Schroter, J., Zahedi, R. P., Hartmann, M., Gassner, B., Gazinski, A., Waschke, J., Sickmann, A., and Kuhn, M. (2010) Homologous desensitization of guanylyl cyclase A, the receptor for atrial natriuretic peptide, is associated with a complex phosphorylation pattern. *FEBS J. 277*, 2440–2453.
26. Bereta, G., Wang, B., Kiser, P. D., Baehr, W., Jang, G. F., and Palczewski, K. (2010) A functional kinase homology domain is essential for the activity of photoreceptor guanylate cyclase 1. *J. Biol. Chem. 285*, 1899–1908.